Modelling Shallow Water Wave Equations

CIV 524 Final Project

Ephraim Bryski

Contents

1 Abstract

A numerical model of small amplitude waves travelling in shallow water was developed using the linear 2-dimensional wave equations. The model was first verified with a 1-dimensional reduction of the equations, modelling travelling waves, wave reflection, and superposition, in addition to comparing the wave speed to theory. The 2-dimensional equations were then used to model diffraction through an opening, and refraction on approaching a decreasing water depth, which was compared to prediction by Snell's Law. While limited, the model was successful in predicting linear phenomena observed at the coast.

2 Model Creation

The 2-dimensional wave equations were used for the model. These equations assume the velocity is uniform across the depth, and is therefore only appropriate for shallow water.

The equations of force balance equate the net force on a water column due to the slope of the water surface with the acceleration of the column:

$$\frac{\partial u}{\partial t} = -g\frac{\partial \eta}{\partial x}$$
$$\frac{\partial v}{\partial t} = -g\frac{\partial \eta}{\partial y}$$

The equations of mass balance equates the influx of water due to the velocity gradient with the change in height:

$$\frac{\partial \eta}{\partial t} = -h_0\left(\frac{\partial u}{\partial x} + \frac{\partial v}{\partial y}\right)$$

These equations were discretized in order to develop a numerical model. A square region was discretized into an MXN grid, as shown in Figure 1, with M being the number of rows, and N being the number of columns. with each grid having an associated water depth. Between neighboring grids is an associated velocity. Neighboring heights are used to update the velocities. For example, $u_{1,2}$ is computed from $\eta_{1,1}$ and $\eta_{1,2}$. This produces an MXN-1 u matrix and M-1XN v matrix. The fixed boundary condition described below makes the velocities on the border 0, producing an MXN+1 u matrix and M+1XN v matrix. Neighboring velocities are then used to update the height. For example, $\eta_{1,1}$ is computed from $u_{1,1}$, $u_{1,2}$, $v_{1,1}$, and $v_{2,1}$. This once again leads to an MXN η matrix. This process is repeated iteratively, allowing for the evolution of the water surface.

The discretized shallow water equations are the following:

$$\frac{\Delta u_{i,j}}{\Delta t} = -g\frac{\eta_{i,j} - \eta_{i,j-1}}{\Delta x}$$

$$\frac{\Delta v_{i,j}}{\Delta t} = -g\frac{\eta_{i,j} - \eta_{i-1,j}}{\Delta y}$$

$$\frac{\Delta \eta_{i,j}}{\Delta t} = -h_0\left(\frac{u_{i,j+1} - u_{i,j}}{\Delta x} + \frac{v_{i+1,j} - vi,j}{\Delta y}\right)$$

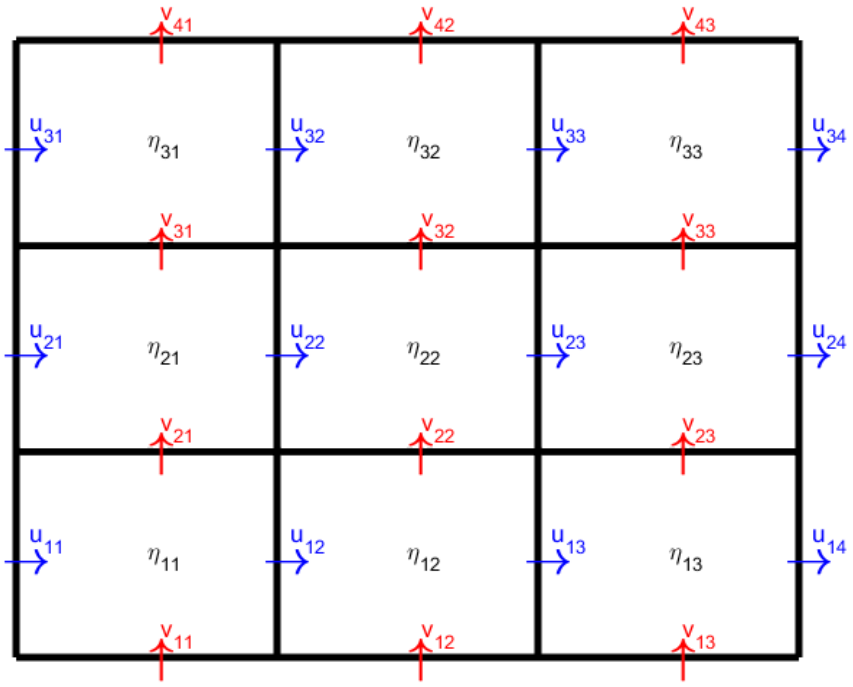

Figure 1: Discretization of a a 2-D region into a 3X3 grid

Fixed boundary conditions were used for all demonstrations.The fixed boundary condition constrains the velocity at the boundary to 0:

$$u_{x=0} = 0$$

$$u_{x=n} = 0$$

$$v_{y=0} = 0$$

$$v_{y=m} = 0$$

Where m and n are the dimensions in the y and x directions, repsectively.

Waves were generated either by modifying the initial water surface for a single wave pulse, or with applying a forced velocity boundary condition for a train of waves. The former was used for the 1-dimensional demonstrations of reflection and superposition, while the latter was used for the 2-dimensional demonstrations of diffraction and refraction.

3 Results and Discussion

3.1 Travelling Waves

Travelling waves were modelled and verified qualitatively using a 1-dimensional region with fixed boundary conditions on either end.

A 1 m wave was produced by generating the surface of a 2 m wave with no velocity on the boundary as seen in Figure 2 (a). This is the position and velocity of a 1 m wave being reflected on the side. As shown in Figure 2 (b) and (c), a 1 m wave is produced from this initial condition and travels without change in shape across the length of the region before being reflected from the opposite side as seen in Figure 2 (d). This process of repeated reflections is repeated indefinitely.

The doubling of wave height upon reflection is in agreement with linear wave theory, as is translation without deformation.

3.2 Wave Speed

The same method for generating waves described above was repeated for three water depths, and therefore three wave speeds. For each depth, the time when the peak of the wave crossed 20 m and 80 m was determined. The actual wave speed was computed by dividing the difference of 60 m by the time taken. The predicted wave speed was computed using the equation for shallow water:

$$c = \sqrt{gh}$$

The wave speed vs. water depth is plotted in Figure 3 and compared with the predicted relation. As shown, the wave speed precisely matches the predicted speed from shallow water linear wave theory.

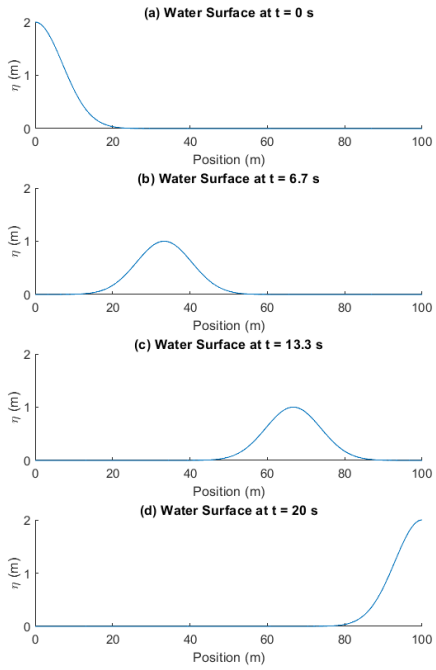

Figure 2: Travelling wave reflecting off the left and right ends, both with fixed boundary conditions

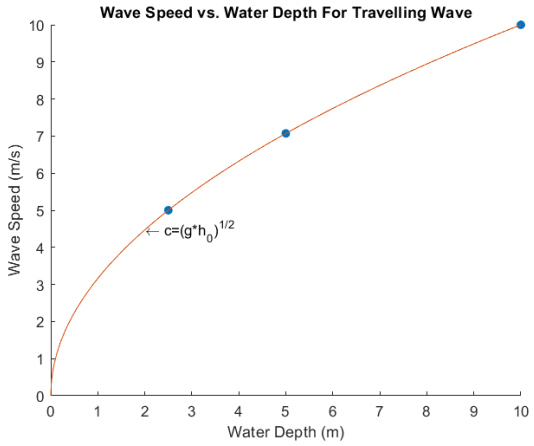

Figure 3: Wave speed vs. water depth as compared with shallow water linear wave theory

3.3 Superposition

The same method used to produce travelling waves was performed with two waves on either end travelling in opposite directions. As seen in Figure 4, the water surface produced when the waves reach the same location is the sum of the two waves. The waves then pass each other without any modification. This is in agreement with shallow water linear wave theory.

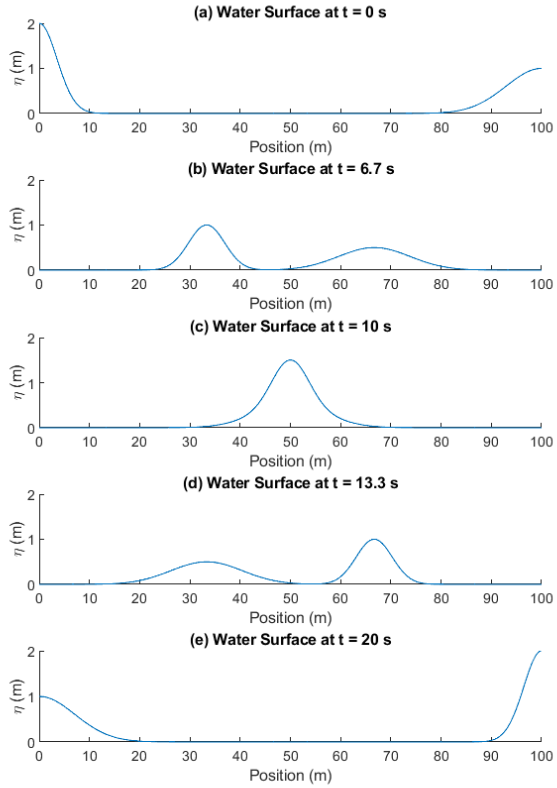

Figure 4: Two waves travelling in opposite directions demonstrating superposition. (a) The two waves are formed by generating the water surface during reflection, (b) The 1 m wave travels to the right and the 0.5 m wave travels to the left, (c) The waves reach the same location producing a 1.5 m wave, (d) The waves pass each other without change in shape, (e) The waves reflect off the opposite sides.

3.4 Diffraction

Diffraction was modelled using a 2-dimensional region and the results were verified qualitatively.

The region for the model is shown in Figure 5. A fixed boundary condition was used for all four sides of the region, except for a 20 m gap at the center of the left side. The fixed boundary condition is marked by thick black lines.

The waves were generated differently than for the 1-dimensional models. The initial water surface was set to 0. Instead, the boundary condition of the 20 m gap was forced, with the velocity varying in time by a sinusoidal function. The equation used was:

$$u = A \sin\left(\frac{2\pi}{T} t\right)$$

Where $A = 8m/s$ and $T = 2s$

This forced velocity, equivalent to a paddle generating waves, produces a train of waves as opposed to a single pulse.

The train of waves propagate through the gap and expand outward in arcs, as shown by the circular bands in Figure 5, representing wave fronts. This circular expansion of waves passing through a gap can be observed in nature when water waves pass through an opening such as the spaces between a series of off-shore breakwaters.

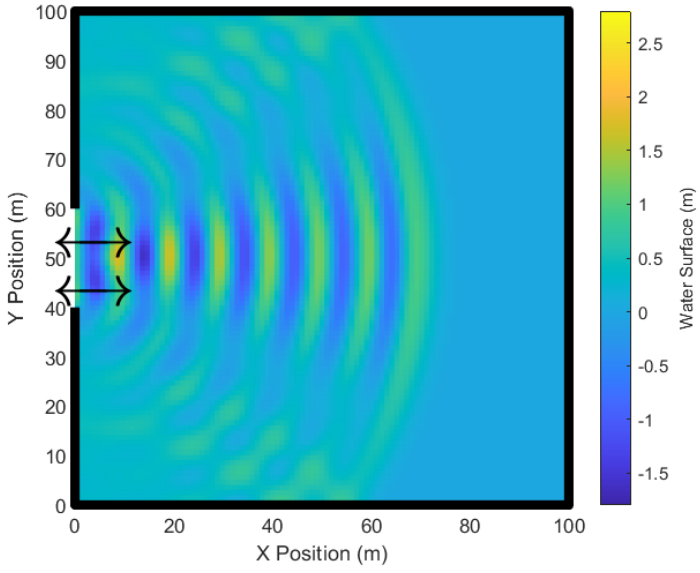

Figure 5: A train of waves pass through a 20 m opening on the left side expand into the region in arcs. The color represents the water surface.

3.5 Refraction

Refraction was modelled using a 2-dimensional region with a non-uniform bathymetry and the resulting refraction was verified with Snell's Law.

Unique to this simulation, the depth was not constant across the region. Instead, there was a bathymetry which was deepest at the bottom left and shallowest at the top right as shown in Figure 6. The equation used for the bathymetry was:

$$h = 3\left(2^{2/3} - \left(\frac{x}{100} + \frac{y}{100}\right)^{2/3}\right)$$

This is the $h = A * y^{2/3}$ bathymetry commonly used to model the coast, but rotated at a 45 degree angle. This was done so that waves travelling directly in the x-direction would be at a 45 degree angle relative to the shore.

The region for the model is shown in Figure 7. A fixed boundary condition was used for top, bottom, and right sides, as shown in thick black lines. The left side has the same forced velocity boundary condition as with diffraction, but with an amplitude of 1 m/s instead of 8 m/s.

As seen in Figure 7, as the waves propagate to the right they bend, the wave front approaching the 45 degree angle of the bathymetry. This refraction can be understood through shallow linear wave theory. At lower water depths, or closer to the shore, the wave speed is lower. By Snell's Law, this causes a change in angle. This is similar to waves at an angle approaching the shore more head-on as they come nearer.

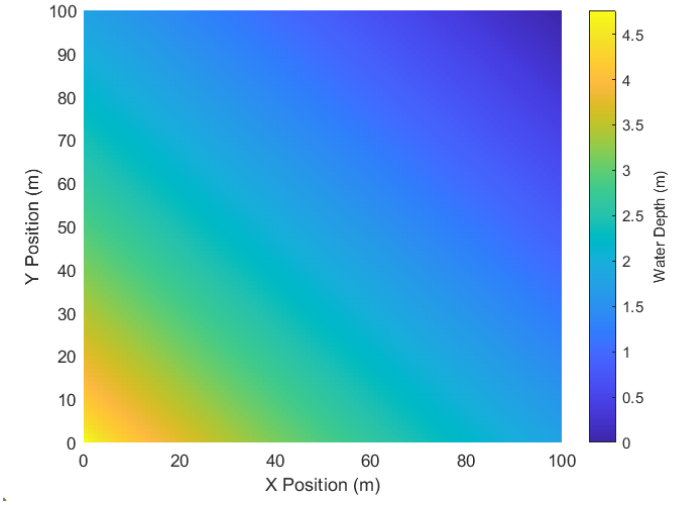

Figure 6: The bathymetry for modelling refraction, with the color representing the depth

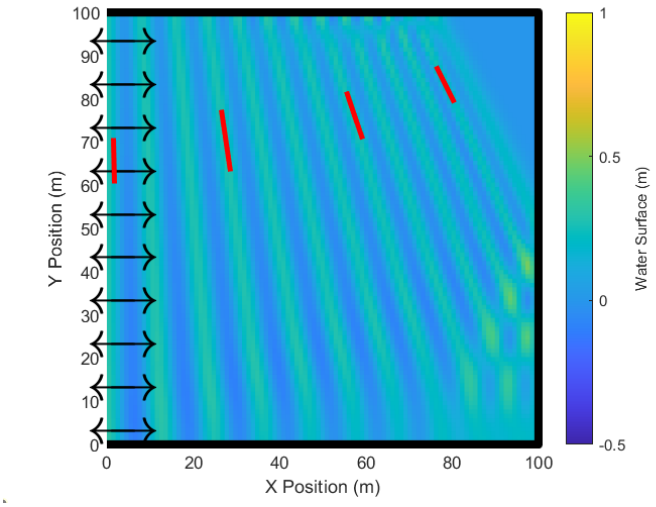

Figure 7: Refraction of a train of waves entering the region with the bathymetry shown above. The red lines indicate where the angle was sampled for verifying Snell's Law.

The refraction observed in the simulation was verified quantitatively using Snell's Law. Four wave fronts were selected as shown by the red lines in Figure 7. The tangent line was produced by manually picking points. The angle relative to contour lines of the bathmetry, or a 45 degree angle between the x and y direction, was used. The location of the wave front was used to determine the water depth by the bathymetry. This depth was then used to determine the wave speed by $c = \sqrt{gh}$. The relation between the sine of the angle and the wave speed is shown in Figure 8. Snell's Law predicts a perfect linear relation. With a root mean square error of only 0.019, it shows fairly close agreement. Possible sources of error included the fixed boundary condition modifying the wave front angle as well as the discretization imperfectly modelling the wave.

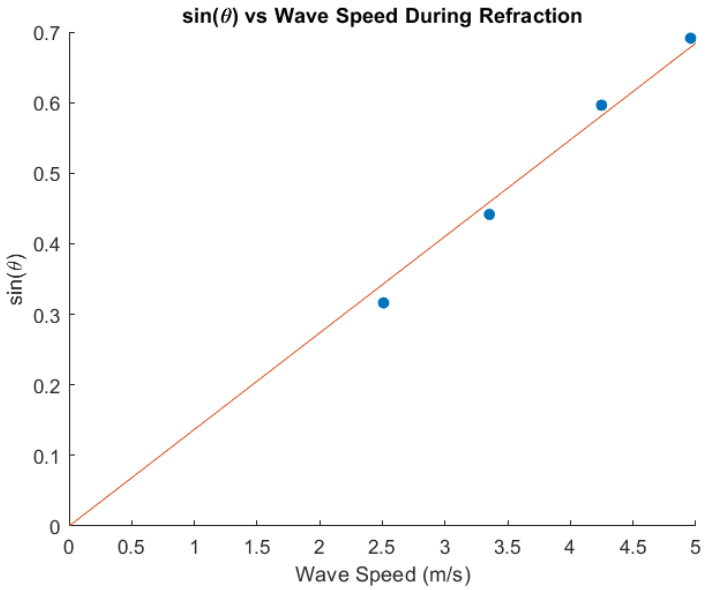

Figure 8: The sine of the angle vs the shallow water predicted wave speed for the four sampled points is plotted and compared with the linear relation predicted by Snell's Law.

4 Conclusion

The model used in this report based off of shallow water linear wave theory was able to accurately model several key phenomena including reflection, superposition, diffraction, and refraction. Setting the initial water surface and a boundary condition with a varying velocity were both used successfully to generate waves. The speed of the wave precisely matched that predicted by the governing wave equations, and refraction was in close agreement with Snell's Law.

The model used is of course limited. It is unable to model wave breaking, longshore currents, Stoke's drift, undertow, and many more important coastal processes which lead to rich complexity actually observed at the shore. Due to these limitations, it is unlikely to be useful as a predictive tool. However, it is an excellent tool for gaining insight into how mathematical models lead to coastal processes. Future work could using more complete mathematical models, including using the general Airy linear wave equation instead of the shallow water simplification to produce more complex 3-dimensional simulations. The effect of adding nonlinearity to the model could also be studied.